Vol 17 No 8, August 2008
1674-1056/2008/17(08)/3083-04

Chinese Physics B

© 2008 Chin. Phys. Soc.
and IOP Publishing Ltd

Fabrication of high-quality submicron Nb/Al–AlO_x/Nb tunnel junctions*

Yu Hai-Feng(于海峰), Cao Wen-Hui(曹文会), Zhu Xiao-Bo(朱晓波),
Yang Hai-Fang(杨海方), Yu Hong-Wei(于洪伟), Ren Yu-Feng (任育峰),
Gu Chang-Zhi(顾长志), Chen Geng-Hua(陈赓华), and Zhao Shi-Ping(赵士平)†

Beijing National Laboratory for Condensed Matter Physics, Institute of Physics, Chinese Academy of Sciences, Beijing 100080, *China*

(Received 16 January 2008; revised manuscript received 25 March 2008)

Nb/Al–AlO_x/Nb tunnel junctions are often used in the studies of macroscopic quantum phenomena and superconducting qubit applications of the Josephson devices. In this work, we describe a convenient and reliable process using electron beam lithography for the fabrication of high-quality, submicron-sized Nb/Al–AlO_x/Nb Josephson junctions. The technique follows the well-known selective Nb etching process and produces high-quality junctions with V_m=100 mV at 2.3 K for the typical critical current density of 2.2 kA/cm^2, which can be adjusted by controlling the oxygen pressure and oxidation time during the formation of the tunnelling barrier. We present the results of the temperature dependence of the sub-gap current and in-plane magnetic-field dependence of the critical current, and compare them with the theoretical predictions.

Keywords: Nb junctions, fabrication, superconducting qubit, macroscopic quantum phenomena
PACC: 7450, 7475, 7490

1. Introduction

Recently, artificial atoms realized using superconducting circuits have attracted much attention not only for their potential quantum computation applications[1−5] but also for the studies of the macroscopic quantum phenomena.[6,7] The key elements of a superconducting circuit are Josephson junctions. Experimentally, the low-T_c materials of aluminium (Al) and niobium (Nb) are most frequently used. While Al junctions are relatively easy to handle during fabrication, Nb junctions have their advantage of being stable against thermal cycling, which is crucial for the practical applications. In addition, the superconducting transition temperature T_c and the energy gap Δ of Nb are 9.25 K and 1.5 meV, respectively, which are higher than 1.2 K and 0.18 meV of Al. From this point of view, the Nb junctions would have larger Josephson coupling energy compared to that of the Al junctions, if their normal-state resistance is the same. The larger Δ of Nb should also be more effective in suppressing possible quasiparticle dissipations.

Nb junctions, in their practical use, often require an adjustable critical current density J_c and a size ranging from microns down to submicrons. J_c can usually be conveniently adjusted by controlling the oxygen pressure and oxidation time during the formation of the tunnelling barrier. On the other hand, junction fabrication processes based on the trilayer technique, such as selective Nb anodization process (SNAP) and selective Nb etching process (SNEP), have been successfully used to produce the micron-sized junctions.[8−13] To fabricate junctions with further reduced size, modified SNAP or SNEP,[14,15] or the shadow evaporation technique,[16] combined with electron-beam lithography (EBL) have been considered by some groups. Chen *et al*, for instance, have successfully used self-aligned process to fabricate high-quality Nb junctions with sizes as small as 0.15 μm.[17]

In this work, we describe a convenient and reliable SNEP-like process for the fabrication of high-quality, submicron-sized Nb/Al–AlO_x/Nb junctions, using EBL to define the junction area (we did not use the anodization process since the resulting Nb-oxides may introduce defects that reduce quantum coherence of the device). Using this process, high-

*Project supported by the National Natural Science Foundation of China (Grant Nos 10474129 and 10534060) and the Ministry of Science and Technology of China (Grant Nos 2006CB601007 and 2006CB921107).
†Corresponding author. E-mail: spzhao@aphy.iphy.ac.cn

quality junctions with area down to $S \sim 0.3\,\mu\text{m}^2$ have been fabricated. We present the results of the temperature dependence of the sub-gap current and in-plane magnetic-field dependence of the critical current for a junction with $S \sim 2\,\mu\text{m}^2$ (V_m=100 mV at 2.3 K and J_c=2.2 kA/cm^2), and compare them with the theoretical predictions.

2. Fabrication process

Our process was SNEP-like and started with the Nb/Al–AlO_x/Nb trilayer preparation. The trilayers were prepared in a DC magnetron sputtering system equipped with a water-cooled rotating substrate table and three sputter targets (of Nb, Al, and Au), each 4 inches in diameter. The base pressure of the vacuum system was 1.0×10^{-6} Pa. The sample holder was made from stainless steel, and was in good contact with the substrate table so that heat could be dissipated quickly. We found that the temperature at the surface of the sample holder could decrease from 100°C down to 40°C in about 1.5 min right after Nb films of 200 nm in thickness were sputtered continuously.

The Nb films were sputtered in high-purity Ar at a pressure of 1.5 Pa. This pressure was chosen to give nearly stress-free Nb films, as found from the x-ray diffraction measurements.[11−13] The films were deposited at a rate of 2.4 nm/s and had a T_c of 9.2 K. To obtain a good quality of the junction barrier, the Al films, 4–7 nm in thickness and sputtered at the rate of 0.4 nm/s, were fabricated about 5 min after the first layer of Nb films was deposited. In this way, the temperature of the Nb films was low enough when the Al films were sputtered, which is important for the continuous coverage of the Al films over the Nb film surface.[18] The junction barrier was formed by oxidizing Al in a load-lock chamber. The barrier's thickness and thus the junction's J_c were controlled by the oxygen pressure and oxidation time at a given temperature. Finally, after oxidation, a 50 nm thick Nb film was fabricated at the same rate in main vacuum chamber.

From the junction area definition, we find it helpful to start with the patterned Nb/Al–AlO_x/Nb trilayers having the same height as the surrounding insulating area. This can be achieved either by sputtering a SiO_2 layer before removing the patterning photoresist (samples described in this work were made in this way) or by etching a depth in the thermally oxidized Si substrate before the preparation of the trilayer. For the latter process, the junction formation can be seen schematically in Fig.1. The starting steps in this case can be described as follows. First a 1 μm thick photoresist layer was spun onto the 25×25 mm^2 thermally oxidized Si substrate. The resist was photolithographically patterned and then post baked. After this, a 200 nm deep structure was formed in the substrate by reactive ion etching (RIE) in the SF_6 and CHF_3 mixing gas. The Nb/Al–AlO_x/Nb trilayers were then deposited. After lift-off in an acetone bath, the patterned trilayers were obtained, which had an approximately the same height as the un-etched substrate surface (see Fig.1).

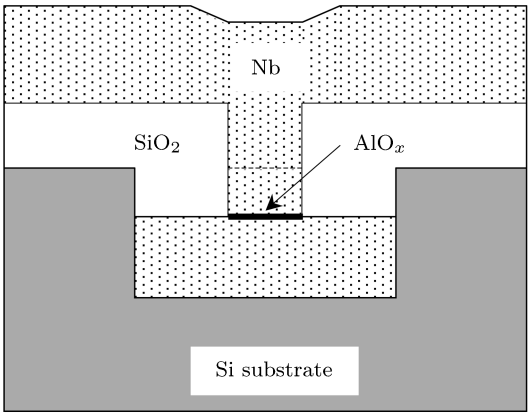


Fig.1. Schematic side view of the Nb/Al-oxide/Nb junctions fabricated using a process described in the text.

The subsequent steps were basically the same for both precesses. Namely, the junction area was defined by using EBL patterning, RIE in the SF_6 plasma to remove the unwanted parts of the top Nb layer, and the deposition and lift-off of an insulating layer of SiO_2 usually with a thickness of 60 nm. Due to the temperature rise during the SiO_2 layer deposition, vigorous ultrasonic agitation was necessary for the lift-off. After this, the contact window was formed. Finally, a 300 nm thick Nb wiring layer was fabricated by EBL patterning and lift-off again. Usually Ar-ion back sputtering was used to clean the trilayer surface in the contact hole before the deposition of the wiring layer.

3. Results and discussions

Figure 2 shows the $I - V$ characteristics of two Nb/Al–AlO_x/Nb junctions fabricated using the above

described techniques. Figures 2(a) and 2(b) show a larger junction with S=1.5×1.5 μm^2 measured at 4.2 K and at 30 mK in a dilution refrigerator, respectively. The critical current (I_c) of the junction is 50 μA, the gap voltage is 2.8 mV, and its spreading is less than 0.1 mV. The quality parameter V_m, defined by the product of the critical current I_c and the subgap resistance R at 2 mV, is ∼100 mV at 2.3 K.

Figure 2(c) shows the $I-V$ curve of a smaller junction with S=0.6×0.6 μm^2 at 4.2 K. It can be seen that the junction quality does not deteriorate as the junction size decreases down to the submicron regime. The smaller I_c compared to the expected value as can be seen in the figure is attributed to the noise in our measurement system, which becomes more influential as the junction's size and I_c become smaller. This can also be seen by comparing Figs.2(a) and 2(b) considering that the measurement noise is much smaller in the dilution refrigerator where shielding and filtering have been carefully considered.

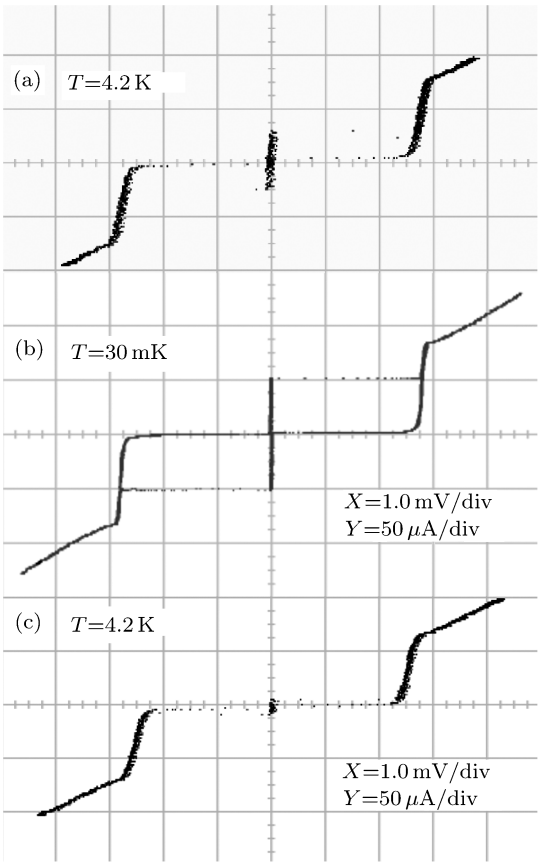


Fig.2. $I-V$ characteristics of two Nb/Al–AlO_x/Nb junctions fabricated in this work. (a) and (b) For a junction with S=1.5 μm×1.5 μm. (c) For a junction with S=0.6 μm×0.6 μm.

To further check the junction quality, we measured the temperature dependence of the sub-gap current I_{gp} and the in-plane magnetic field dependence of I_c. Figure 3 shows the temperature dependence of I_{gp} measured at 1.0 mV for the junction shown in Figs.2(a) and 2(b) (symbols). An in-plane magnetic field on the order of 2×10^{-2} T was used to suppress the Josephson current. We have compared the experimental results with those predicted by the BCS theory for the quasiparticle tunnelling current using the following expression:

$$I_{gp} = \frac{1}{eR_N}\int_{-\infty}^{\infty} N(E)N(E-eV) \times [f(E-eV)-f(E)]\mathrm{d}E, \quad (1)$$

where R_N is the junction's normal-state resistance, $N(E)$ is the BCS density of states of the superconductors, and $f(E)$ is the Fermi distribution. The calculated results are shown as a solid line in the figure. In the calculation, we assumed that the two electrodes of the junction are identical, having an equal Δ=1.4 meV at T=0 K. It can be seen that the experimental data follow the calculated ones closely down to about 3 K, but below this temperature, they start to saturate. It is presently unclear whether the saturation results from the junction's remaining leakage current or the noise in the measurement system.

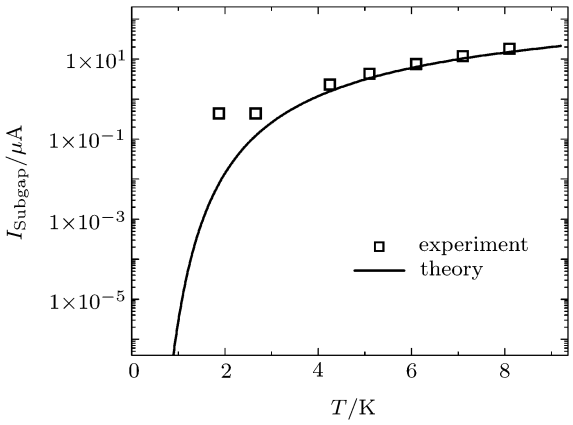


Fig.3. Temperature dependence of the sub-gap current I_{gp} measured at 1.0 mV (symbols) for the junction shown in Figs.2(a) and 2(b) with the Josephson current suppressed by a parallel magnetic field. The solid line is the BCS prediction obtained by numerical integration of Eq.(1).

For a Josephson junction with highly spatial uniform electrodes and barriers, its I_c versus in-plane magnetic field B would show the familiar Fraunhofer diffraction pattern. This I_c-B dependence is de-

scribed by

$$I\left(\frac{\phi}{\phi_0}\right) = I_c \left| \frac{\sin \pi \frac{\phi}{\phi_0}}{\pi \frac{\phi}{\phi_0}} \right|, \qquad (2)$$

where ϕ is the magnetic flux through the junction's barrier region and ϕ_0 is the flux quantum. The $I_c - B$ dependence measured at 4.2 K for the junction shown in Figs.2(a) and 2(b) is shown in Fig.4 (symbols), together with the prediction from Eq.(2) (line). The good agreement between experiment and theory indicates the high degree of uniformity in the junction area.

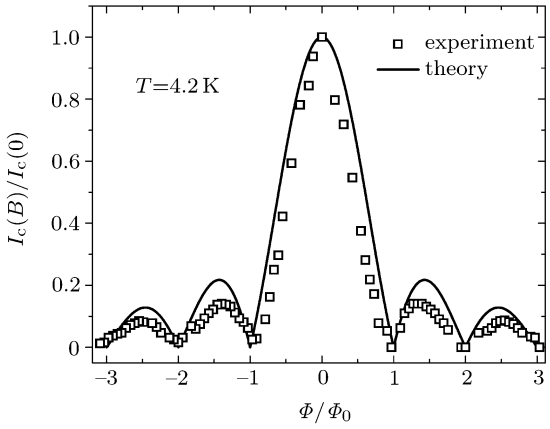


Fig.4. Critical current vs. parallel magnetic field measured at 4.2 K for the junction shown in Figs.2(a) and 2(b), showing the familiar Fraunhofer diffraction pattern.

4. Conclusion

We have successfully developed a reliable and reproducible process to fabricate high-quality submicron Nb/Al–AlO_x/Nb tunnel junctions following the well-known SNEP technique and using EBL to define the junction area. The junction's J_c can be adjusted by the oxidation parameters of the tunnelling barrier. Junctions with quality parameter of V_m=100 mV at 2.3 K and area as small as 0.3 μm^2 have been fabricated. These Nb/Al–AlO_x/Nb junctions should be useful in their quantum computing applications and for the studies of the macroscopic quantum phenomena.

Acknowledgments

We thank Wei Chen and Siyuan Han for many helpful discussions.

References

[1] Nakamura Y, Pashkin Yu A and Tsai J S 1999 *Nature* **398** 786
[2] Vion D, Aassime A, Cottet A, Joyez P, Pothier H, Urbina C, Esteve D and Devoret M H 2002 *Science* **296** 886
[3] Chiorescu I, Nakamura Y, Harmans C J P M and Mooij J E 2003 *Science* **299** 1869
[4] Van der Wal C H, Ter Haar A C J, Wilhelm F K, Schouten R N, Harmans C J P M, Orlando T P, Lloyd S and Mooij J E 2000 *Science* **290** 773
[5] Yu Y, Han S, Chu X, Chu S I and Wang Z 2002 *Science* **296** 889
[6] Friedman J R, Patel V, Chen W, Tolpygo S K and Lukens J E 2000 *Nature* **406** 43
[7] Martinis J M, Devoret M H and Clarke J 1987 *Phys. Rev.* B **35** 4682
[8] Kroger H, Smith L N and Jillie D W 1981 *Appl. Phys. Lett.* **39** 280
[9] Gurvitch M, Washington M A and Huggins H A 1981 *Appl. Phys. Lett.* **42** 472
[10] Imamura T and Hasuo S 1988 *J. Appl. Phys.* **64** 1586
[11] Du H, Zhao S P, Wang R F, Xu F Z, Chen G H and Yang Q S 1998 *Chin. J. Low Temp. Phys.* **20** 406
[12] Zhao S P, Du H, Chen G H and Yang Q S 1998 *Appl. Phys. Lett.* **72** 3062
[13] Du H, Zhao S P, Wang R F, Xu F Z, Wang J, Chen G H and Yang Q S 1999 *Chin. J Low Temp. Phys.* **21** 1
[14] Bao Z, Bhushan M, Han S and Lukens J E 1995 *IEEE Trans. Appl. Supercond.* **5** 2731
[15] Meng X F, Zheng L Z, Wong A and Van Duzer T 2001 *IEEE Trans. Appl. Supercond.* **11** 365
[16] Hyunsik I, Pashkin Yu A, Yamamoto T, Astafiev O, Nakamura Y and Tsai J S 2006 *J. Korean Phys. Soc.* **48** 1560
[17] Chen W, Patel V and Lukens J E 2004 *Microelectronic Engineering* **73** 767
[18] Blamire M G and Evetts J E 1985 *Appl. Phys. Lett.* **46** 1181